# Laminar Plumes from a Line Source and Their Possible Flow Behaviours.

**Abstract**

Laminar plumes that under goes buoyancy reversal had just been investigated with the assumption that water density was taken as a quadratic function temperature by means of a computational model. We considered a parabolic velocity profile at the source and flow parameters $Re = 100$, $Pr = 11.4$ and varying Froude number within $0.2 \leq Fr \leq 5$. Our results appears very similar to previously studied cases. There was head detachment behaviour and a sideways flapping and vertical bobbing motion after the core of the fountain were exposed. At the fountains core, profiles of vertical velocity component show that decrease in vertical velocity with height is not smoother even at higher Froude numbers as compared to those of our previous study for ($Re = 50$). Our empirically determined scalings laws for fountain height and time to attain maximum height (Eqs 14 & 15) were obtained and are fairly similar with previous results where negative buoyancy is only by means of mixing. Initially rising plumes were symmetric and takes much longer time to attain a fully developed stage as compared to our previous studies. As Froude number increases, the plumes with less buoyancy rises more slowly and could attain greater height before sufficient dense fluid is produced to halt their rise as compared to those with greater buoyancy (smaller Froude numbers). Generally, we can conclude that with the quadratic dependence relation assumption and except for the behaviour in the profiles of vertical velocity component that show some slight differences as compared to those by [3] and the Froude number that represents the balance between inertia and buoyancy forces (responsible for the variation in the fountains heights). Irrespective of the flow parameters used within the Reynolds number range $50 \leq Re \leq 100$ and Prandtl number $Pr = 7 \,\&\, 11.4$ the flow behaviour remains the same.

**Keywords:** Cold water, Line plume, Buoyancy reversal, Numerical simulation.

## 1 Introduction

Buoyancy driven flows are of great interest based on the possibility of buoyancy reversal especially in rising plumes in cold fresh water; which may be due to the nonlinear relation between temperature and density in water. If we introduce a warm water discharge at the bed of a lake or somewhere close to it, where the ambient dense fluid is considered to be quiescent with its temperature below the temperature of maximum density (approximately $4°C$) in fresh water. Mixing is bound to occur between the two fluid (warm water and ambient cold water) which will in turn produce water that is denser than both the warm discharge and the ambient fluid, a process called cabbeling by Foster [1] as also recorded in [3]. In this, it is expected that a plume of warm water which at first rises due to its greater buoyancy may experience buoyancy reversal and form a fountain as the most dense mixed fluid descend to the lake bed: see Fig. 1. More so, if the medium into consideration dose not have greater depth, then the most buoyant fluid could rise to the lake surface and spread outwards forming surface gravity current. But then, further entrainment of cold water into the gravity current will then lead to buoyancy reversal as a result of cabbeling, and the gravity current will halt even as the most dense fluid descend to the lake bed forming a fountain: see Fig. 2. Details of such flow scenarios can also be found in [2] so as to gain more insight.

Power station cooling water discharges are practical examples of such scenarios where flows of this nature can be found. This cooling water is usually discharged at a temperature approximately $10°C$ above that of the ambient water [ 3, 4, 5]. This implies that the warm discharge will definitely be less dense than that of the ambient fluid and as a result of this, the less dense fluid will initially form a rising plume. But then, if the surrounding fluid is below the temperature of maximum density, buoyancy reversal due to cabbeling will occur [3]. At that point, mixed fluid close to the temperature of maximum density will then descend to the floor. In a particular investigation, Hoglund and Spigarelli [6] were able to observe water at a temperature of $5.7°C$ at the bed of lake Michigan in the vicinity of a power station outfall while the natural ambient temperature was $0.5°C$, and concluded that the relatively warm but dense water had been formed by this means. Meanwhile, it is supposed that power station warm discharges will obviously be fully turbulent but then, laboratory experiments from those by Bukreev and Gusev [7] could produce plumes with much lower Reynolds numbers, meaning that such flows may be laminar or in transition to turbulence. However, previous authors have also carried out thorough investigation on both laminar and turbulent fountains in the usual condition of linear dependence relation of density on temperature, with a negatively buoyant fluid being injected upwards into a less dense ambient [3]. These authors [8, 9] have also carried out direct simulation using computational models for axisymmetric and two-dimensional laminar fountains to determine linear relations of the form $Z_m/x_0 = a_0 + a_1 Fr$ between the final, steady fountain height $z_m$ and the source Froude number $Fr = V_0/(x_0 g_0')^{1/2}$ in the range $0.2 \leq Fr \leq 1$ [3]. Where $x_0$ is the half-width of a line source or the radius of an axisymmetric source, $V_0$ is the mean velocity and $g_0'$ is the reduced gravity at the source, and the numerical coefficients $a_0$ and $a_1$ depend on the source geometry (axisymmetric or line source) and velocity profile [3]. These authors were also able to determine linear relations for the fountain width, and a quadratic relation of the form $t_m/(x_0/V_0) = b_0 + b_2 Fr^2$ for the time $t_m$ taken to establish the steady fountain height. Though, the computations were for fixed Prandtl number $Pr = 7$ and Reynolds number $Re = 200$. Later computational study where these parameters were varied [10] showed that $Z_m/x_0 = a_0 + a_1 Fr Re^{-1/2}$ and similarly for fountain width, provided the $Re \leq 200$. Whereas, fountain height and width became independent of Reynolds number at larger values of $Re$ [3].

With a uniform velocity profile at the fountain source, Srinarayana et al. [11] in their study also showed that the fountain remained steady and symmetric only up to $Fr \approx 2.25$. But as Froude numbers increases, lateral oscillations (a flapping motion) were found; these were periodic for $Fr \leq 4$ but chaotic for $Fr > 4$. The scaling for the fountain height was $Z_m/x_0 \sim Fr^{1.15}$ in the periodic oscillation regime, and $Z_m/x_0 \sim Fr^{4/3}$ with chaotic flapping [3]. Afterwards, these authors [12] considered a parabolic source velocity profile and obtained different figures of the transition Froude numbers, and a $Fr^2$ scaling for fountain height in the periodic flapping regime [3]. Experimentally studied cases by Srinarayana et al. [13] and Williamson et al. [14] also showed a wider range of fountain behaviours, and that transitions between the possible behaviours are also dependent on both Froude and Reynolds numbers. Similarly, [15] have also

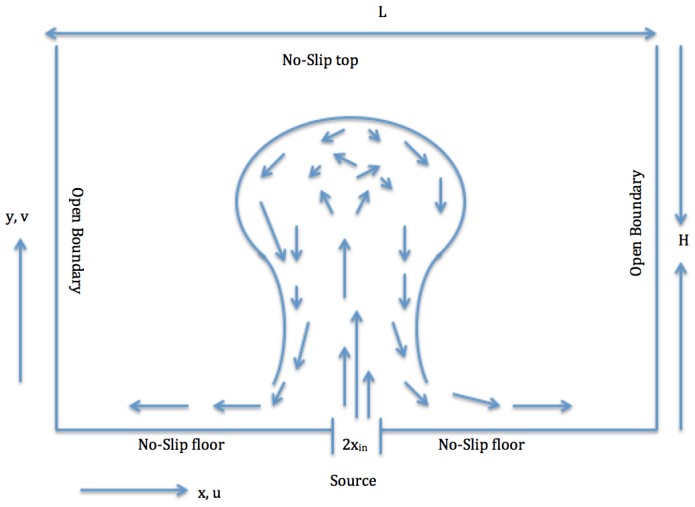


Fig. 1: Schematic of plume with buoyancy reversal, also showing domain for computations.

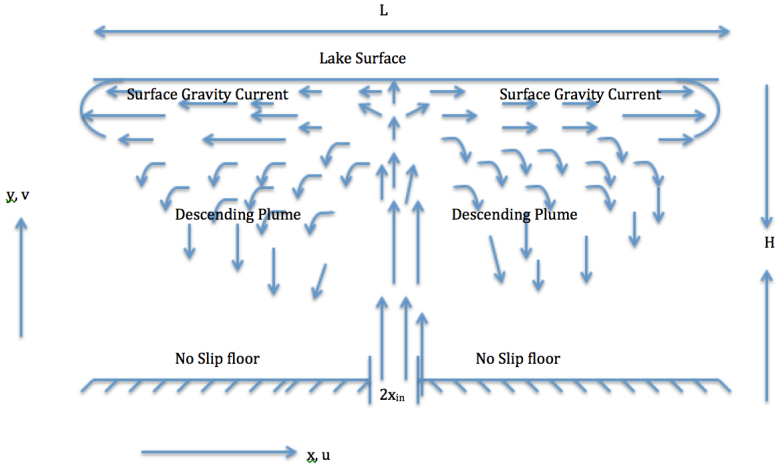


Fig. 2: Schematic of plume reaching lake surface before experiencing buoyancy reversal.

reported on the dependence of fountain height on both Froude and Reynolds numbers experimentally. However, it is also clear that the above reviewed cases have all considered flows where the buoyancy flux opposes the momentum flux at the source; whereas, there has been less attention given to fountains arising from buoyancy reversal [3]. Buoyancy reversal requires a nonlinear relation between density and the mixing ratio of discharged and ambient fluids: assuming density to be a quadratic function of mixing ratio, with the mixed fluid less dense than the mean of the constituents densities [3] These authors [16] also used the entrainment assumption of Morton, Taylor and Turner [17] in a model of a dense fluid injected upwards into a less dense ambient. However, this process is comparable to that of a warm water being injected downwards into an ambient colder than the temperature of maximum density, where the plume may form an inverted fountain or may continue downwards without being arrested as the case may be [3]. Kay [18] in his work studied this case as well as the upwards injection of warm water into a cold ambient, again using the classical entrainment assumption. The difficulty here is that it can model a plume up to the level where it is arrested, but cannot really justify that of the reversed flow in a fountain [3]. The experimental study by Bukreev and Gusev [7] involved the injection of warm water upwards into an ambient below the temperature of maximum density at low Reynolds number, so that a laminar fountain was produced; as in the turbulent case studied by Turner [19]. Both authors noted a periodic oscillations of the fountain height, and that as time progresses, the descending dense water would be displaced to one side of the rising plume. But then, they only gave few examples without any systematic investigation of how the flow depends on source conditions [3].

It is worth nothing that we have also considered laminar fountains with the assumption that density was taken as a quadratic function of temperature numerically. At the source, the discharge has a parabolic velocity profile, with fixed Reynolds number $Re = 50$, Prandtl number $Pr = 7$ and varied Froude number over the range $0.2 \leq Fr \leq 2.5$. Our results show some similarities to those fountain resulting from injection of a negatively buoyant fluid upward into a less dense ambient. The plume is initially symmetric, but then its head detaches as it approaches its maximum height. The detached head is denser than the fluid in the plume below it, and the interaction between the sinking head and the rising plume causes a sideways deflection. This process led to a side- to-side flapping motion and vertical bobbing. As Froude number increases, the growth rate of the plume became slower, but the plume eventually reaches a greater height, and our empirically determined date could only allow us to identify a single regime of Froude number dependence of fountains height. But then, Srinarayana et al. [11] identified three regimes of Froude number dependence for the height of their fountains, reflecting qualitative differences in behaviour (e.g. between steady and unsteady flow) in different ranges of $Fr$. In contrast, we have not found such differences in behaviour, which have triggered the present investigation. Thus, the aim of this paper is to further carryout a computational investigation with this assumption, whether there is a different regime for $Fr > 2$. Laminar plumes which do not reach the surface of the ambient water body, but form fountains due to buoyancy reversal is our interest. The ambient is assumed to be a quiescent and homogeneous body of water, colder than the temperature of maximum density. Warm water, initially less dense than the ambient, is injected at constant speed from a line orifice in the base of the container, so the flow is assumed two-dimensional [3]. We keep the Reynolds and Prandtl numbers fixed through out the simulations, $Re = 100$ and $Pr = 11.4$, and vary the Froude number $0.2 \leq Fr \leq 5$ which represents the balance between inertia and buoyancy forces. The choice of $Pr = 11.4$ is more appropriate especially for the power station warm discharge in cold fresh water, where mixing will certainly produce mixture at $T_m$.
Computational domain length and height will be kept constant, where length $L = 70x_{in}$, i.e., $0 \leq X \leq 70$, and a domain height $H = 56x_{in}$ i.e., $0 \leq Y \leq 56$. We also assume open sides and rigid, no-slip top and base, except for the orifice with width $2x_{in}$ at the centre of the domain base, where the warm fluid is expected to be injected at mean velocity $v_{in}$ as we have in Fig. 1 [3].

## 2 Model Formulation and Governing Equations

The behaviour of laminar plumes which do not reach the surface of the ambient water body, but form fountains due to buoyancy reversal is being considered. This is very important and possible because of the

nonlinear relation between density $\rho$ and temperature $T$. Thus, the relation below is useful for this study,

$$\rho = \rho_m - \beta(T - T_m)^2 \tag{1}$$

This, we think gives an appropriate fit to the experimentally determined density of fresh water at temperature below $10^{\circ}C$ if we consider $T_m = 3.98^{\circ}C$, $\rho_m = 1.000 \times 10^3\ kg.m^{-3}$ and $\beta = 8.0 \times 10^{-3}\ kg.m^{-3}(^{\circ}C)^{-2}$ [3, 20, 21] and all other fluid properties (e.g. viscosity, thermal diffusivity) are assumed constant. We also assume that the flow is time dependent and two dimensional, and that the liquid property is constant except for the water density, which changes with temperature and in turn results to the buoyancy force. The velocity profile at this plume source is assumed parabolic as for laminar Poiseuille flow (cf. [11]),

$$v(x,0) = \frac{3}{2} v_{in}[1 - (\frac{x}{x_{in}})^2] \tag{2}$$

The input fluid temperature is $T_{in}$ is assume constant at the centre of the domain and a uniform initial ambient temperature $T_\infty$. For dimensionless variables, the difference between the ambient and the $T_m$ gives a normal temperature scale, while the source conditions provide the only length and velocity scales. The domain dimensions are not suitable length scales, as they are taken to be large enough for conditions at the sides and top of the domain to have no effect on the plume. Thus, we non-dimensionalise the coordinates $x$, $y$, velocity components $u$, $v$, time $t$, pressure $p$ and temperature $T$ by

$$U = \frac{u}{v_{in}} \quad V = \frac{v}{v_{in}} \quad X = \frac{x}{x_{in}} \quad Y = \frac{y}{x_{in}} \quad \tau = \frac{t}{x_{in}/v_{in}} \quad P = \frac{p}{\rho v_{in}^2} \quad \phi = \frac{T - T_\infty}{T_m - T_\infty}, \tag{3}$$

where $x$ and $u$ are horizontal, $y$ and $v$ are vertical [2].
We can also define our dimensionless parameters, the Reynolds $Re$, Prandtl $Pr$ and Froude $Fr$ numbers, by

$$Re = \frac{v_{in} x_{in}}{\nu}, \quad Pr = \frac{\nu}{\alpha}, \quad Fr^2 = \frac{\rho_m v_{in}^2}{g\beta(T_m - T_\infty)^2 x_{in}}, \tag{4}$$

where $\nu$ and $\alpha$ are the respective diffusivities of momentum and heat, $\nu = \mu/\rho$ and $\alpha = k/\rho c_p$. Where, $\mu$ is viscosity, $k$ is thermal conductivity and $c_p$ is specific heat capacity. In terms of these dimensionless variables and parameters, the continuity equation, the horizontal and vertical momentum equations and the thermal energy equation are given as:

$$\frac{\partial U}{\partial X} + \frac{\partial V}{\partial Y} = 0 \tag{5}$$

$$\frac{\partial U}{\partial \tau} + U\frac{\partial U}{\partial X} + V\frac{\partial U}{\partial Y} = -\frac{\partial P}{\partial X} + \frac{1}{Re}(\frac{\partial^2 U}{\partial X^2} + \frac{\partial^2 U}{\partial Y^2}) \tag{6}$$

$$\frac{\partial V}{\partial \tau} + U\frac{\partial V}{\partial X} + V\frac{\partial V}{\partial Y} = -\frac{\partial P}{\partial Y} + \frac{1}{Re}(\frac{\partial^2 V}{\partial X^2} + \frac{\partial^2 V}{\partial Y^2}) + \frac{1}{Fr^2}[\phi^2 - 2\phi] \tag{7}$$

$$\frac{\partial \phi}{\partial \tau} + U\frac{\partial \phi}{\partial X} + V\frac{\partial \phi}{\partial Y} = \frac{1}{RePr}(\frac{\partial^2 \phi}{\partial X^2} + \frac{\partial^2 \phi}{\partial Y^2}) \tag{8}$$

Our initial conditions are an undisturbed, homogeneous medium as also given in [2].

$$U = 0, \quad V = 0, \quad \phi = 0, \quad for \quad \tau < 0 \tag{9}$$

For $\tau \geq 0$ we have boundary conditions as follows. On the side walls:

$$\frac{\partial U}{\partial X} = 0, \quad \frac{\partial V}{\partial X} = 0, \quad \frac{\partial \phi}{\partial X} = 0 \quad at\ X = \pm\frac{L}{2x_{in}} \tag{10}$$

At the plume source:

$$U = 0, \quad V(X,0) = 1.5(1 - X^2), \quad \phi = \phi_{in} \quad for\,|X| \leq 1 \quad at\,Y = 0 \tag{11}$$

Elsewhere on the floor of the domain:

$$U = 0, \quad V = 0, \quad \frac{\partial \phi}{\partial Y} = 0, \; for \quad |X| > 1 \quad at\,Y = 0 \tag{12}$$

At the top of the domain:

$$U = 0, \quad V = 0, \quad \frac{\partial \phi}{\partial Y} = 0\,at\,Y = \frac{H}{x_{in}} \tag{13}$$

Reynolds number $Re = 100$ and Prandtl number $Pr = 11.4$ will be fixed throughout this investigation varying Froude number $0.2 \leq Fr \leq 5$. The dimensionless temperature $\phi_{in} = 2.5$ at the centre, and this is equivalent to a warm discharge at $10^{\circ}C$ into an ambient temperature at $0^{\circ}C$. Numerical solution of the above equations is by means of COMSOL Multiphysics software. This commercial package uses a finite element solver with discretization by the Galerkin method and stabilisation to prevent spurious oscillations. We have used the "Extremely fine" setting for the mesh. Time stepping is by COMSOL's Backward Differentiation Formulas [3]. Further information about the numerical methods is available from the COMSOL Multiphysics website [22]. Results will be illustrated mainly by surface temperature plots of dimensionless temperature on a colour scale from dark red for the ambient temperature $\phi = 0.0$, through yellow to white for the source temperature $\phi = 2.5$. Note that $\phi = 1.0$ corresponds to the temperature of maximum density. Meanwhile, $\phi = 2$ correspond to the temperature at which warm water has the same density as that of the ambient cold water [3].

## 3 Results

The following figures $3, 4, 5, 6, 7, 8$ *and* $9$, (with panels (a), (b), (c), (d) respectively of the figures) show the evolution of plumes with different Froude numbers $Fr = 1, 3, 4$ *and* $5$; fixing other flow parameters Reynolds number $Re = 100$ and Prandtl number $Pr = 11.4$. After the release of warm discharge at the source, fluid in the plume with the greatest buoyancy ($Fr = 1$) is becoming dense and approaching its maximum height within the time frame $\tau = 5$ ( see Fig. 3a) as compared to those in the other panels. At this point, cabbeling had begun even though significant amount of dense fluid had not been noticed on the floor. As time progresses, is obvious that plumes with the greatest buoyancy have attained their maximum height and collapsed. This indicates that plumes with higher source Froude numbers rise more slowly, but later attain greater maximum heights. Though, all the plumes will definitely stop rising, having begun to lose momentum as a result of cabbeling [3]. Fig. (4a & 5a) shows that at $\tau = 20$ & $40$ a significant amount of dense fluid has already been shed from the outside of the plume with $Fr = 1$ and spreading outwards on the floor. However, plumes with higher Froude numbers have less vigorous mixing and as such they appear symmetric up to $\tau = 20$ which account for their maximum rise heights (see Fig. 3 & 4). As time further progresses, all the plumes lose their symmetric shape through a process of head detachment (Figs. 5b,& c; 6c & d; 7c & d; 8d). This was as a result of the fact that the head of the plume becomes denser than the neck beneath it, and so rises more slowly which in turn resulted in the process of head detachment. After then, there was an interaction between the sinking detached head and the faster rising fluid in the neck which in turn also causes the head to be deflected from one side to the other [3].

Having that the supply of warm fluid from the source and the production of dense fluid by mixing are a continuous processes; this resulted to a continuous flapping and bobbing motion of the plume (i.e., the sideways deflection of detaching heads results in side-to-side flapping, and the exposure of the plume's core after each head is detached leads to vertical bobbing) [3]. The behaviours as presented are very similar to our previous work [3], where we have considered Reynolds and Prandtl numbers fixed through out the

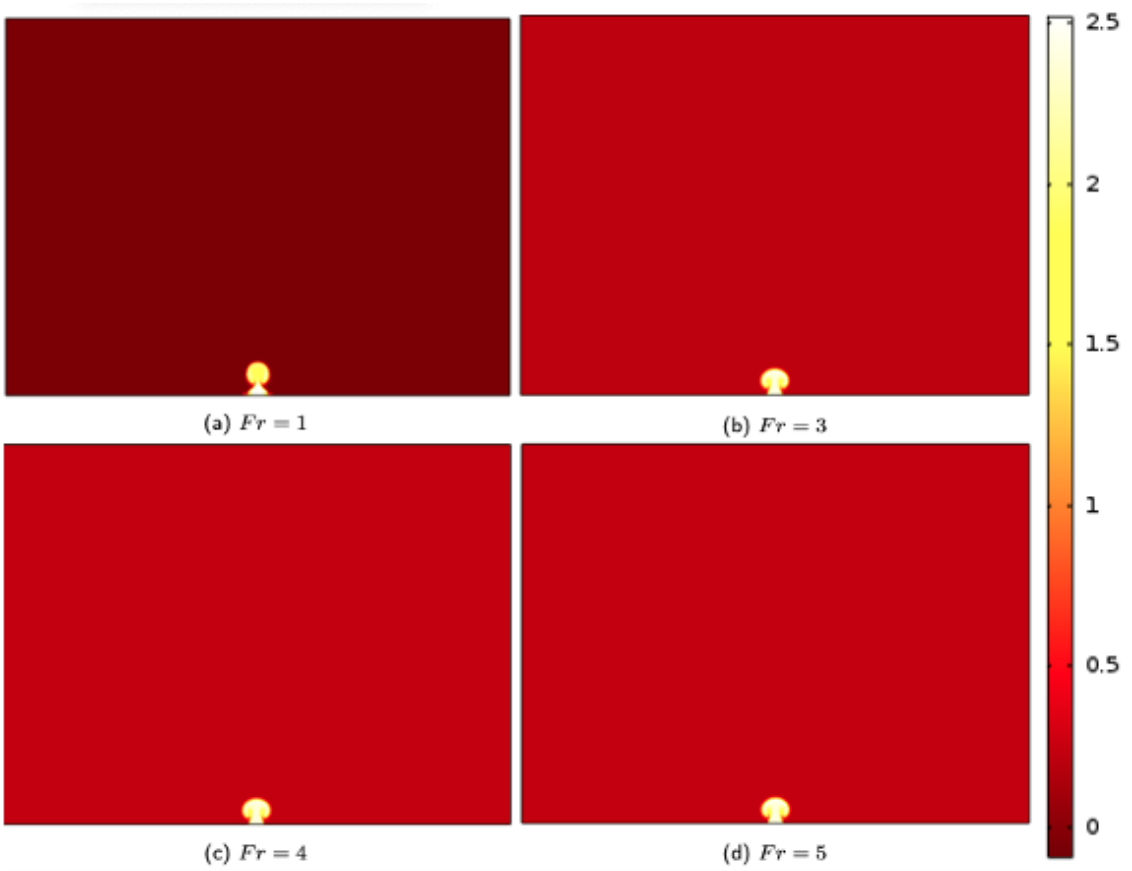


Fig. 3: Temperature field at time $\tau = 5$ for plumes with $Re = 100$, $Pr = 11.4$, $\phi_{\text{in}} = 2.5$ and (a) $Fr = 1$, (b) $Fr = 3$, (c) $Fr = 4$ and (d) $Fr = 5$.

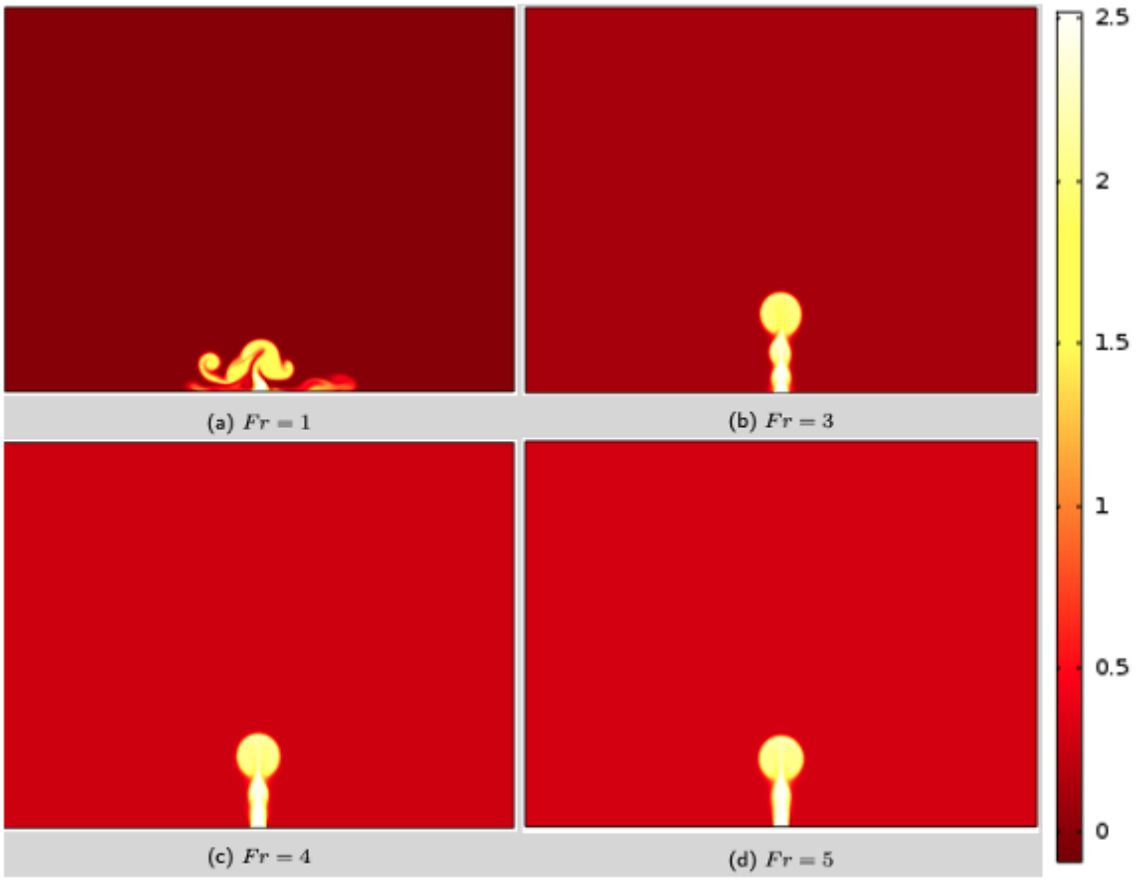


Fig. 4: Temperature field at time $\tau = 20$ for plumes with $Re = 100$, $Pr = 11.4$, $\phi_{\text{in}} = 2.5$ and (a) $Fr = 1$, (b) $Fr = 3$, (c) $Fr = 4$ and (d) $Fr = 5$.

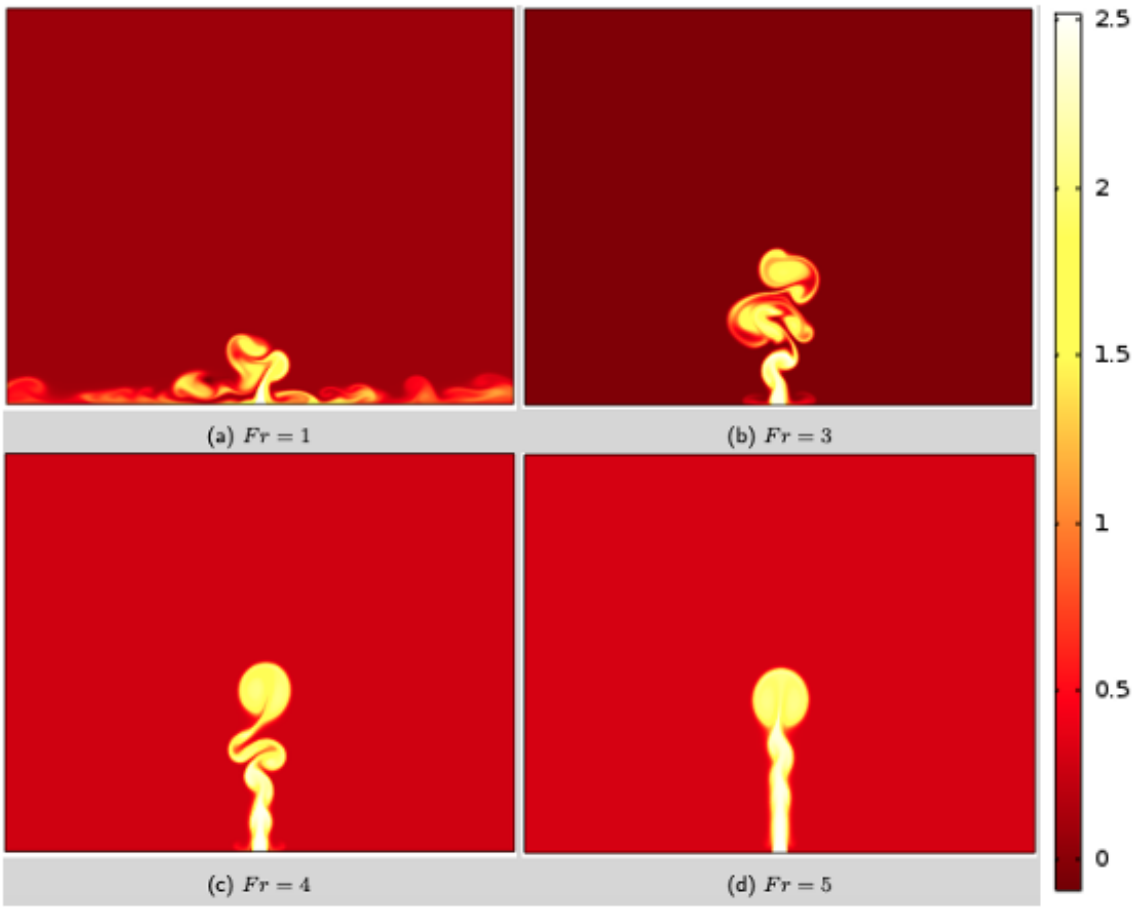


Fig. 5: Temperature field at time $\tau = 40$ for plumes with $Re = 100$, $Pr = 11.4$, $\phi_{\text{in}} = 2.5$ and (a) $Fr = 1$, (b) $Fr = 3$, (c) $Fr = 4$ and (d) $Fr = 5$.

simulations, $Re = 50$ and $Pr = 7$, and vary the Froude number $0.2 \leq Fr \leq 2.5$ so as to carryout a comparative analysis with those by Srinarayana et al. [11]. In that investigation, we were able to record approximately all the behaviours as we have observed here despite the fact that there is a variation in the flow parameters. However, both flapping and bobbing motion has also been recorded by Vinoth and Panigrahi [23] in non-Boussinesq laminar fountains at higher Froude numbers. Results by Srinarayana et al. [11] for a laminar plane fountain with $Fr = 8$ and a linear dependence of density on temperature have also shown some similarities with our case here, especially in the case of the flapping from side to side behaviour. For that of the vertical bobbing behaviour, Turner [19] in a turbulent plume with reversing buoyancy have also recorded that [3]. Whereas, the dense fluid on the floor spread outwards horizontally as density current (see Fig. 4a, 5a, 6a, 7a, 8a & b, 9a & b). This part also appears similar to those by George & Osaisai [24, 25, 26]. Though, the motion in the gravity current in this present investigation is slow, which may be due to the small density difference between the current and the ambient. The spread of the current is steady except when it is perturbed by the arrival of new dense fluid from a detached head, which may cause oscillations downstream: unlike [24 - 26] where the perturbation is as a result of the development of kelvin-Helmholtz instabilities at the interaction layer between the current and the ambient

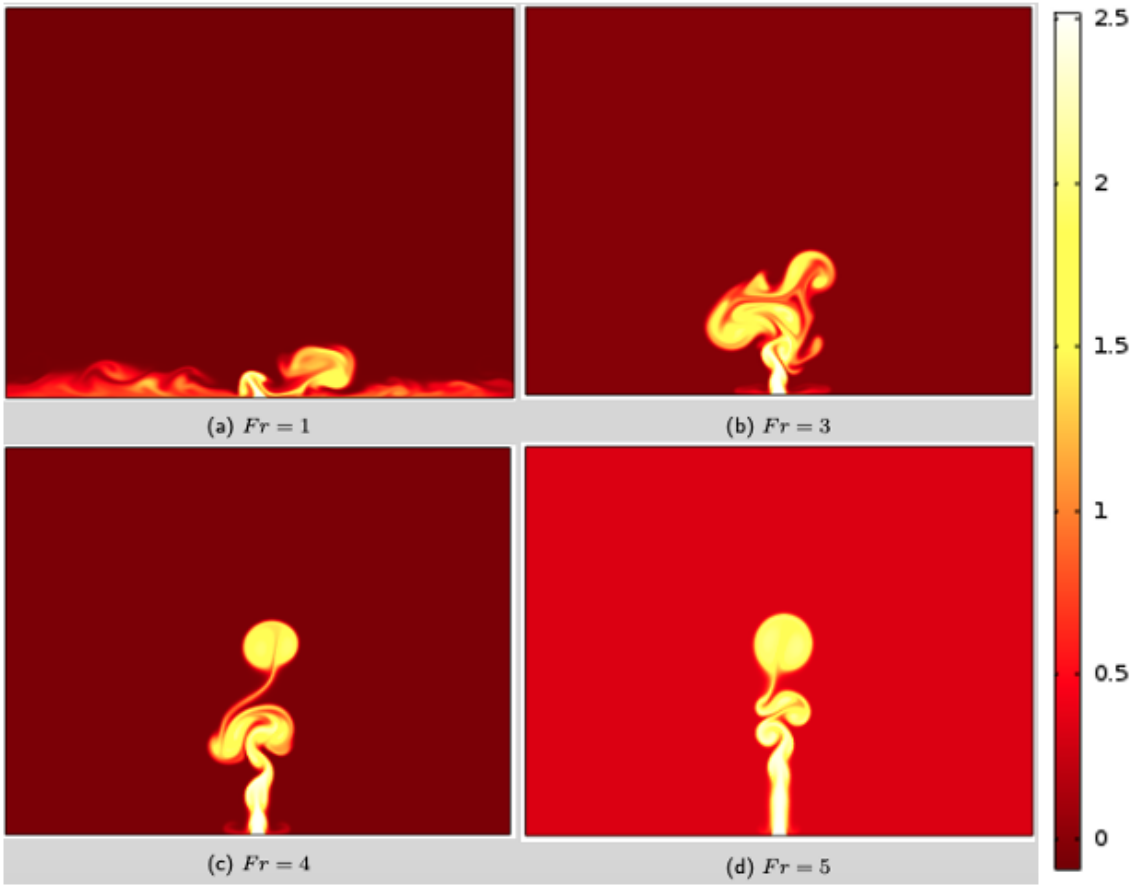


Fig. 6: Temperature field at time $\tau = 50$ for plumes with $Re = 100$, $Pr = 11.4$, $\phi_{\text{in}} = 2.5$ and (a) $Fr = 1$, (b) $Fr = 3$, (c) $Fr = 4$ and (d) $Fr = 5$.

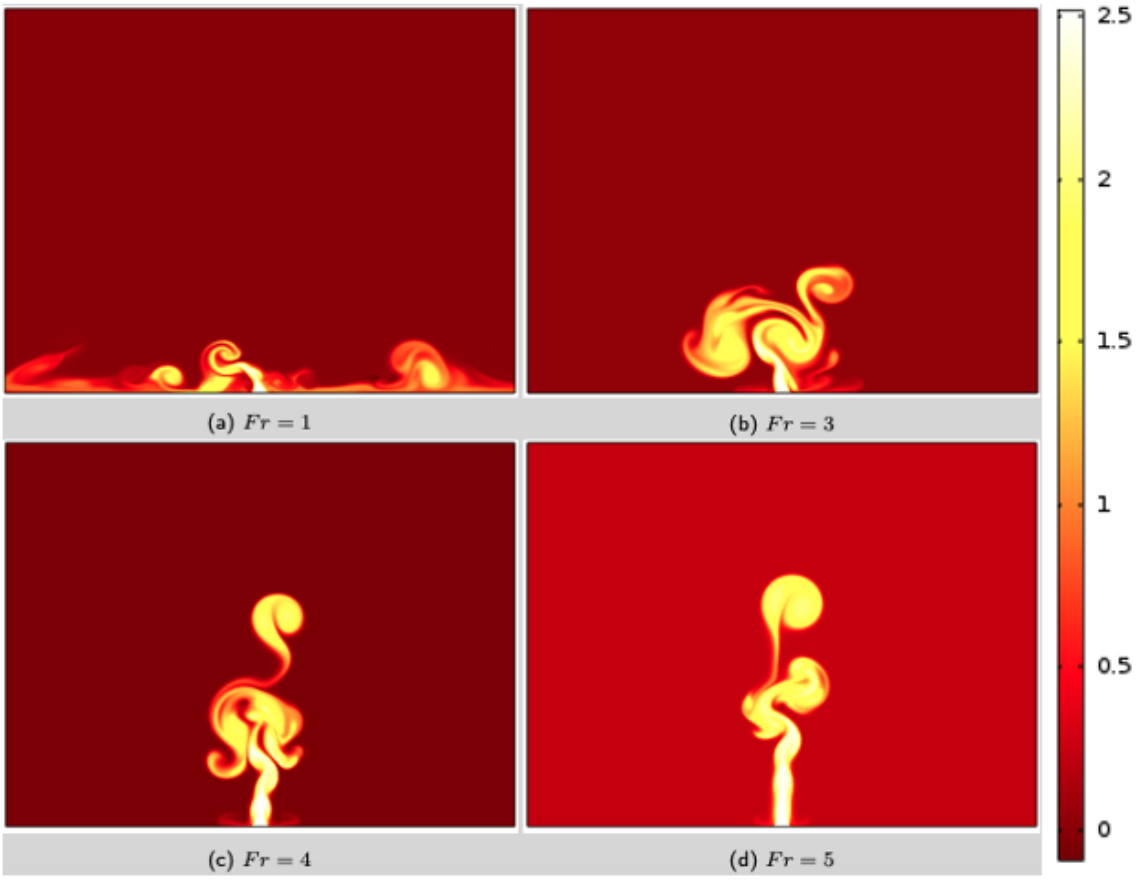


Fig. 7: Temperature field at time $\tau = 60$ for plumes with $Re = 100$, $Pr = 11.4$, $\phi_{\text{in}} = 2.5$ and (a) $Fr = 1$, (b) $Fr = 3$, (c) $Fr = 4$ and (d) $Fr = 5$.

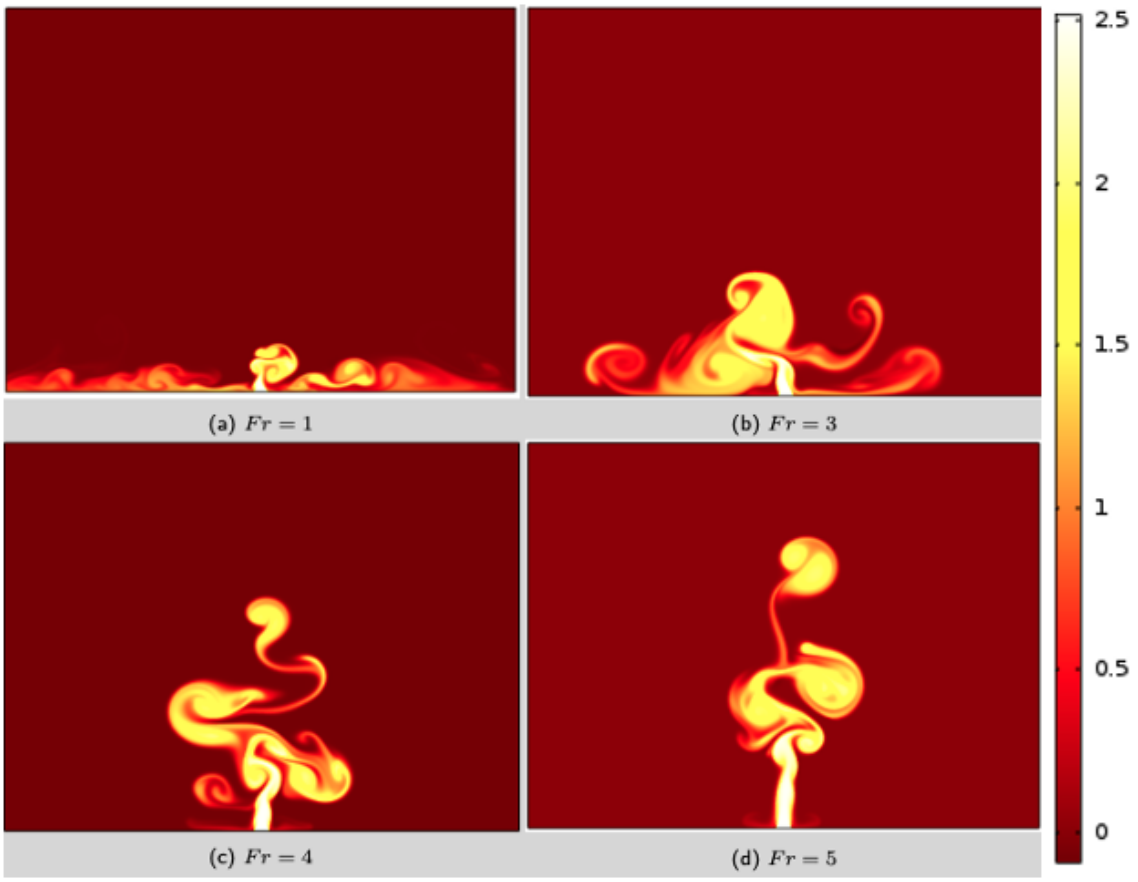


Fig. 8: Temperature field at time $\tau = 80$ for plumes with $Re = 100$, $Pr = 11.4$, $\phi_{\text{in}} = 2.5$ and (a) $Fr = 1$, (b) $Fr = 3$, (c) $Fr = 4$ and (d) $Fr = 5$.

fluid.

Profiles of temperature and the various velocity components up the centre-line of the plume (X = 0) have also been considered in Fig. 10, 11 & 12 which will enable us to gain more insight in such flows. Figure 10 show the profiles of temperature for the four Froude number cases at five different levels. These profiles agree to the fact that plumes with higher Froude number could penetrate the ambient fluid to attain a greater heights: though, at much later time. Whereas, there was vigorous mixing leading to a reduced penetration height for plumes with smaller Froude numbers: though, heights of the various plumes decreases after maximum penetration. Furthermore, there is a region of almost uniform temperature immediately above the source (except for the smallest Froude number) [3]. This indicates that warm water could still be retained even up to that level because of the slow mixing rate and in turn enhances more penetration. From the profiles, it is also clear that decrease in temperature with height is not monotonic. There are fluctuations in these profiles that reaches a local maximum before decreasing sharply to the ambient tem-

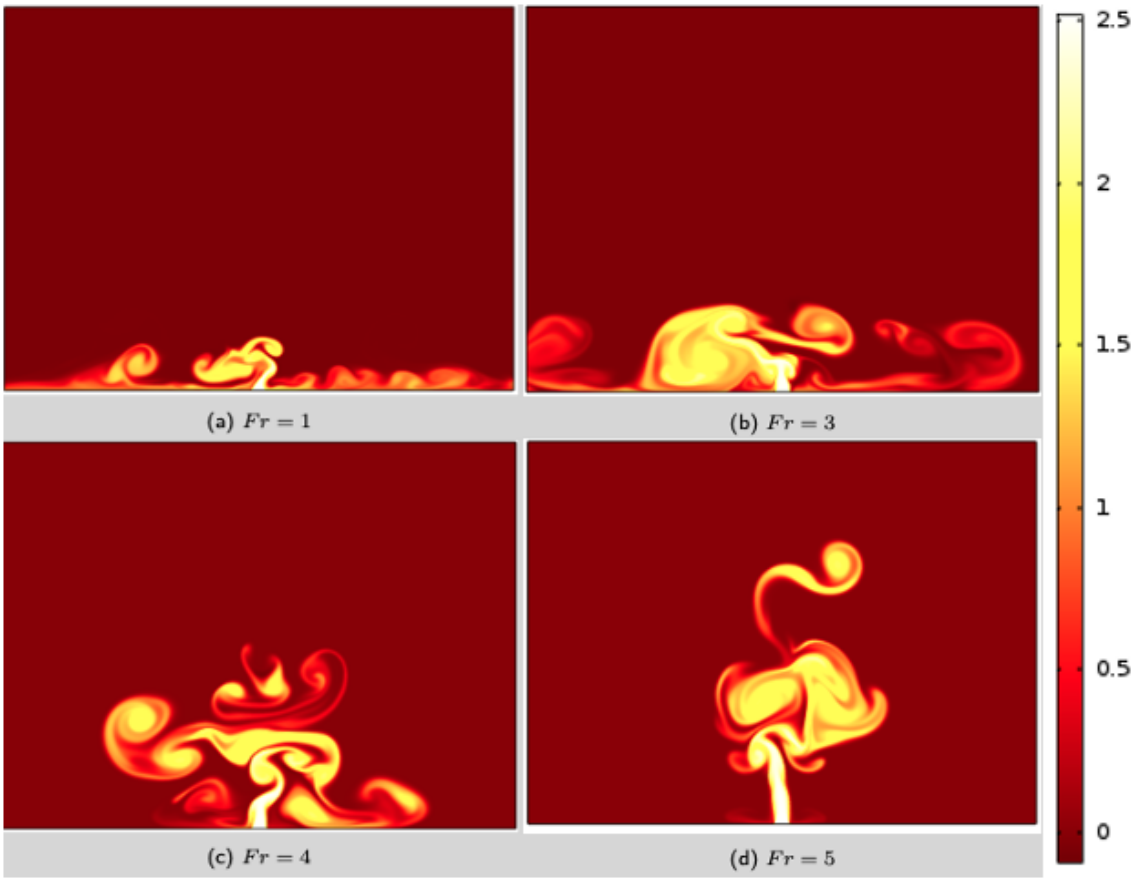


Fig. 9: Temperature field at time $\tau = 100$ for plumes with $Re = 100$, $Pr = 11.4$, $\phi_{\text{in}} = 2.5$ and (a) $Fr = 1$, (b) $Fr = 3$, (c) $Fr = 4$ and (d) $Fr = 5$.

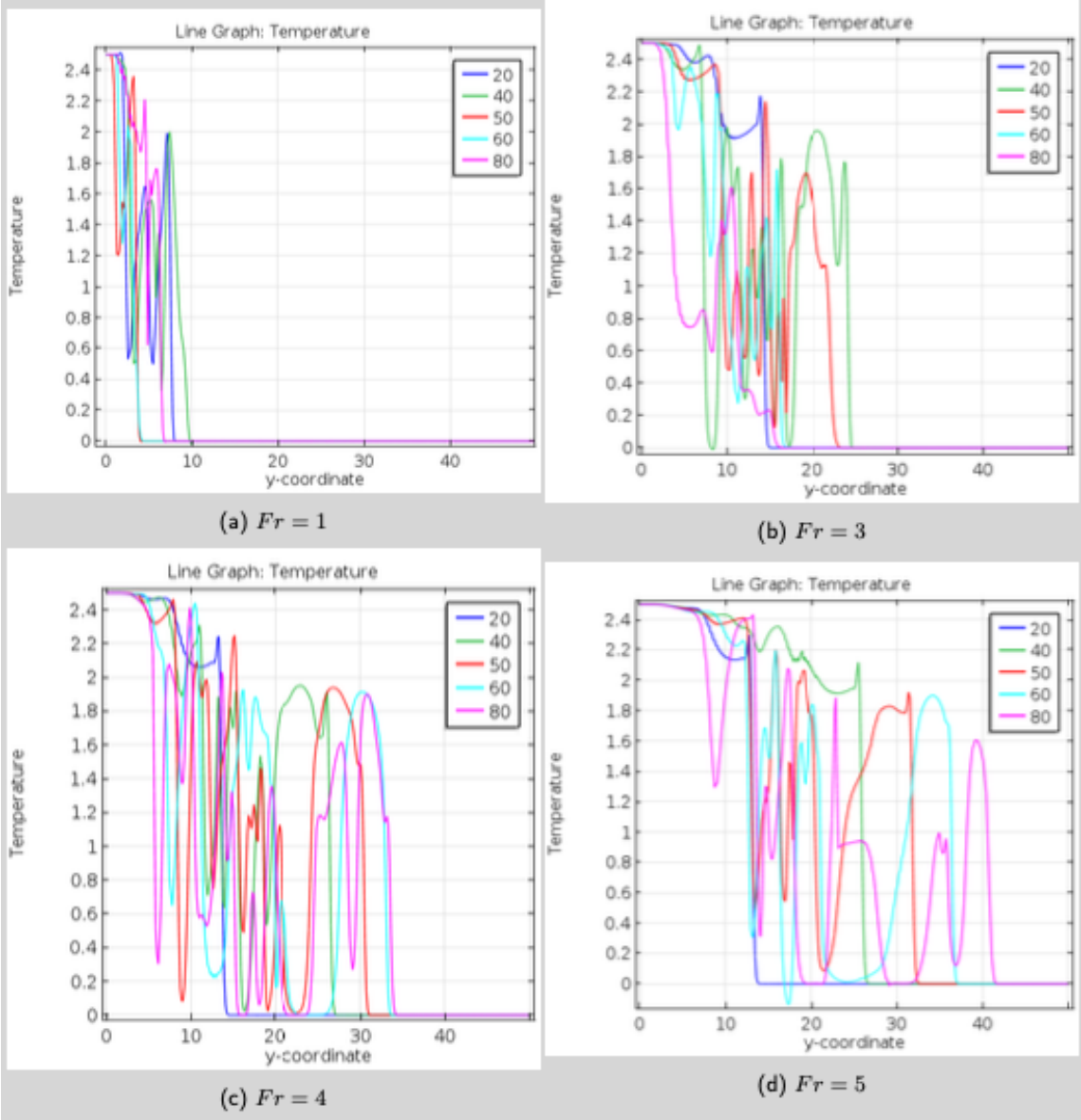


Fig. 10: Dimensionless centreline temperature distribution $\phi(0, y)$ at times $\tau = 20, 40, 50, 60, 80$, for plumes with $Re = 100$, $Pr = 11.4$, $\phi_{\text{in}} = 2.5$ and (a) $Fr = 1$, (b) $Fr = 3$, (c) $Fr = 4$ and (d) $Fr = 5$

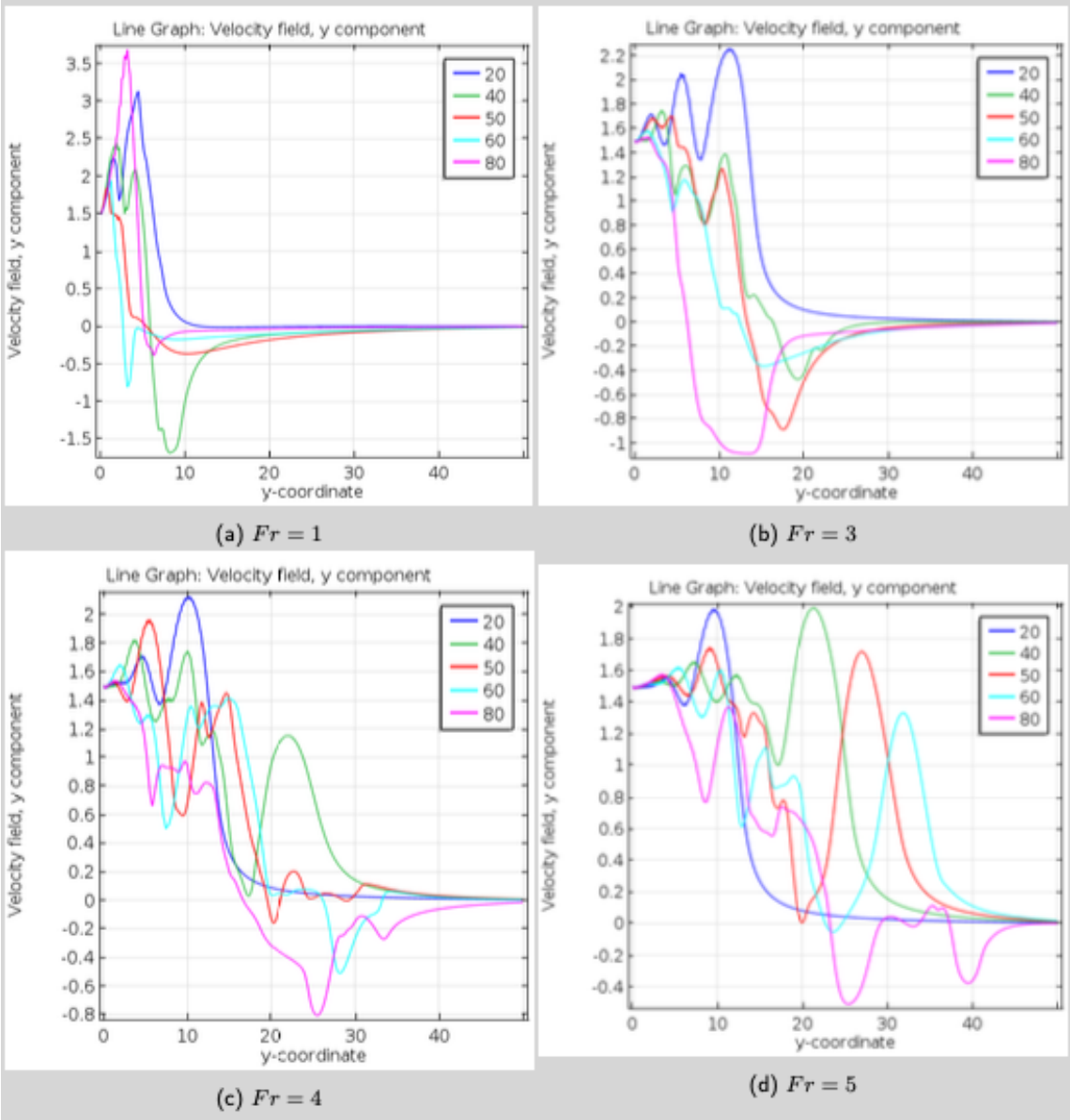


Fig. 11: Dimensionless centreline Y-component velocity distribution $V(0, y)$ at times $\tau = 20, 40, 50, 60, 80$, for plumes with $Re = 100$, $Pr = 11.4$, $\phi_{\text{in}} = 2.5$ and (a) $Fr = 1$, (b) $Fr = 3$, (c) $Fr = 4$ and (d) $Fr = 5$

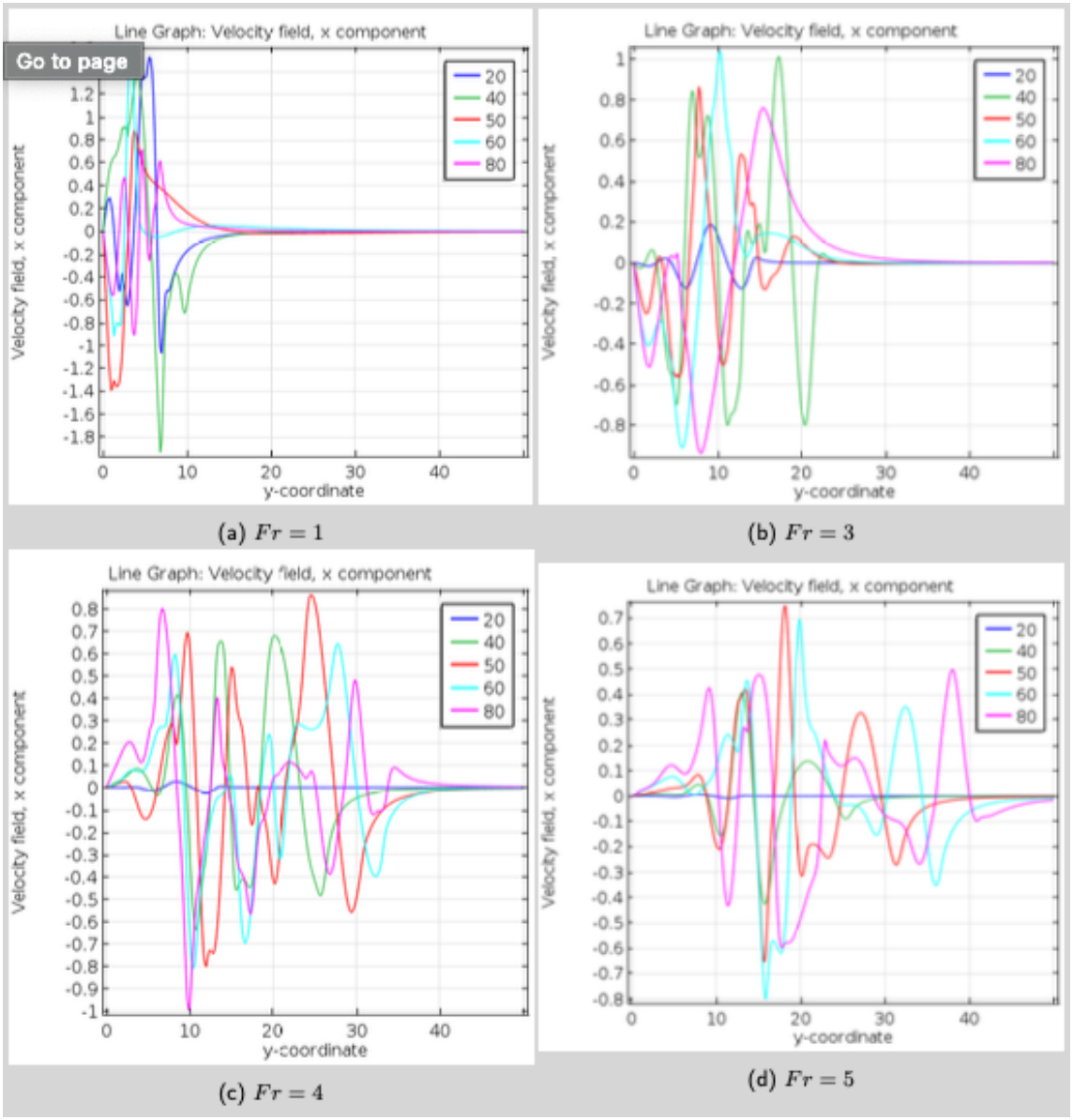


Fig. 12: Dimensionless centreline X-component velocity distribution $U(0, y)$ at times $\tau = 20, 40, 50, 60, 80$, for plumes with $Re = 100$, $Pr = 11.4$, $\phi_{\text{in}} = 2.5$ and (a) $Fr = 1$, (b) $Fr = 3$, (c) $Fr = 4$ and (d) $Fr = 5$

perature at the plume's top [3].
Profiles of vertical velocity component are shown in Fig. 11; which indicates some sort of intense fluctuations ranging from the source with some degree of downward velocities within some time interval. Where the downward velocities indicates descending fluid and this behaviour is common to all the Froude number cases considered. There is a significant difference in the profiles of vertical velocity component as compared to those by [3]. There results show that at higher Froude numbers the decrease in vertical velocity with height is smoother, but still involves some degree of fluctuation with some level of downward velocities within the upper part of the plume after it has reached its maximum height and starts to sink. Whereas, even at higher Froude numbers the decrease in vertical velocity with height is not smoother in this present study which might result from the slight increase in Reynolds number that might have enhanced slightly intense mixing as compared to the former. Profiles of horizontal velocity component up the plume centreline are also shown in Fig. 12. These profiles show that there is a strong side-to-side flapping motion close to the source within the time range considered. Though, as Froude numbers increases this side-to-side flapping motion takes little longer time to develop and is less intense but penetrate to a greater heights.

We have considered the maximum rise height $Z_n$ attained by the plume and the time $\tau_n$ taken to attain that height and tabulated for a range of Froude numbers as shown in Table 1, and plotted in Figs. 13 and 14. The results as recorded here also appears very similar to those by George & Kay [3] where, they could only identify a single regime of Fr-dependence similar to what we have also recorded here. This we have shown by the straight lines in Figs. 13 and 14, representing the best fit power laws obtained by linear regression of $\log Z_n$ and $\log \tau_n$ on $\log Fr$ from our empirically determined data set: where $R^2$ is the regression coefficient in each case.

$$Z_n = 8.9394 Fr^{0.9063} \qquad [R^2 = 0.9888] \tag{14}$$

$$\tau_n = 10.461 Fr^{1.1841} \qquad [R^2 = 0.9953], \tag{15}$$

As regards the main focus of this present study, the Froude number range as considered has not guaranteed a different regime of flow. But then, Srinarayana et al. [11] in their work could identify three regimes of Froude number dependence for the fountain's height, which reflect the differences in behaviour (e.g. between steady and unsteady flow) in different ranges of $Fr$. Though, they have assumed a linear dependence of density on temperature. One of the unique behaviours with the quadratic dependence assumption is head detachment. In some cases with higher Froude numbers, this detached head could penetrate farther. Having observed this, we are suggesting that much smaller values of Reynolds number and a moderate value of Froude number be reconsidered to know if these behaviours are entirely depended on flow parameters for the laminar flow scenario. Above all, we can conclude here that with the quadratic dependence relation assumption of density on temperature, and except for the behaviour in the profiles of vertical velocity component that show some slight differences as compared to those by [3] and the Froude number that represents the balance between inertia and buoyancy forces (responsible for the variation in the fountains heights). Irrespective of the flow parameters used within the Reynolds number range $50 \leq Re \leq 100$ and Prandtl number $Pr = 7 \,\&\, 11.4$ the flow behaviour remains the same.

## 4 Summary/Conclusion

The behaviour of laminar plumes had just been investigated with a quadratic dependence relation assumption by means of a computational model. Time taken to attain a fully developed stage appears longer as compared to our previous studies. As Froude number increases, the plumes with less buoyancy rises more slowly and could attain greater height before sufficient dense fluid is produced to halt their rise because of

Table 1: Maximum plume height $Z_n$ and time taken to reach that height at Froude numbers $0.2 \leq Fr \leq 5$

| Fr | $\tau_n$ | $Z_n$ | Fr | $\tau_n$ | $Z_n$ | Fr | $\tau_n$ | $Z_n$ |
|---|---|---|---|---|---|---|---|---|
| 0.2 | 1.8 | 2.55 | 2.5 | 27.6 | 18.978 | 4.8 | 73.5 | 40.314 |
| 0.5 | 4.6 | 4.8 | 2.8 | 33.6 | 21.504 | 5.0 | 75.6 | 42.524 |
| 0.8 | 7.8 | 6.938 | 3.0 | 36.0 | 22.59 | | | |
| 1.0 | 10.0 | 8.051 | 3.2 | 41.0 | 24.697 | | | |
| 1.2 | 12.6 | 9.905 | 3.5 | 47.0 | 27.512 | | | |
| 1.5 | 16.6 | 12.706 | 3.8 | 52.0 | 31.025 | | | |
| 1.8 | 19.6 | 14.77 | 4.0 | 56.6 | 33.241 | | | |
| 2.0 | 22.6 | 16.233 | 4.2 | 63.0 | 34.681 | | | |
| 2.2 | 24.6 | 17.46 | 4.5 | 67 | 37.987 | | | |

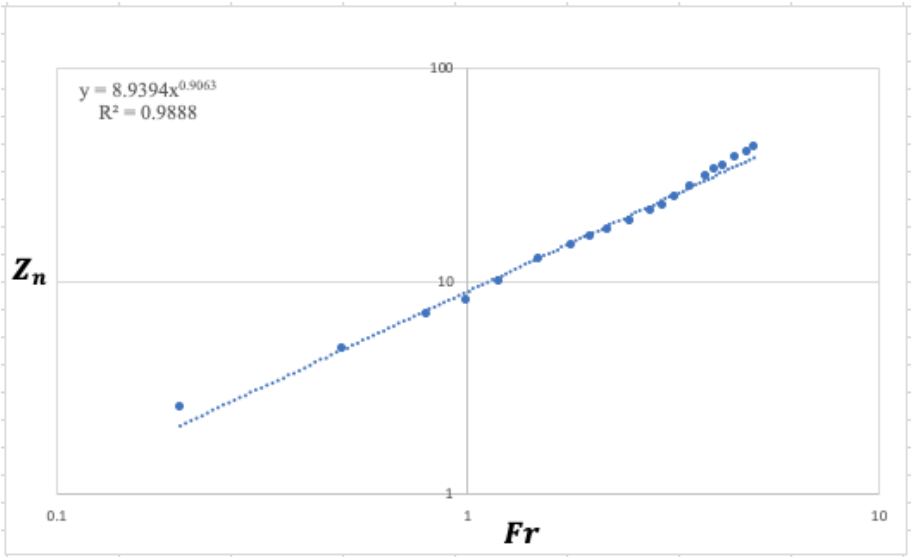


Fig. 13: Variation of maximum plume height with Froude number

their slower mixing rate as compared to those with greater buoyancy (smaller Froude numbers). Mixture here require just little mixing to attain buoyancy reversal. Initially, the plumes were symmetric but later display a sideways flapping and vertical bobbing after the core of the fountain were exposed. This seem to be the effect of head detachment after the frontal head had become dense and displaces the plume sideways and sink. At the fountains core, profiles of vertical velocity component show that decrease in vertical velocity with height is not smoother even at higher Froude numbers; which might result from the slight increase in Reynolds number ($Re = 100$) that might have enhanced slightly intense mixing as compared to those of our previous study for ($Re = 50$) [3]. Dense fluid on the floor spread outwards as gravity current. Our empirically determined scalings laws for fountain height and time to attain maximum height (Eqs 14 & 15) are also fairly in line with those by [3] where negative buoyancy is only by means of mixing. They are also to some extent similar to those by [27] for very weak fountains $Z_n \propto Fr^{\frac{2}{3}}$ and $\tau_n \propto Fr^{\frac{4}{3}}$. However, the mechanism for halting the rise of the plume differs between our case and that of laminar fountains with the linear dependence relation assumption: whereas fountains have negative buoyancy regardless of any mixing. This might be the reason for not justifying a separate regime in our case here. One of the unique behaviours with the quadratic dependence assumption is head detachment. Having observed that with

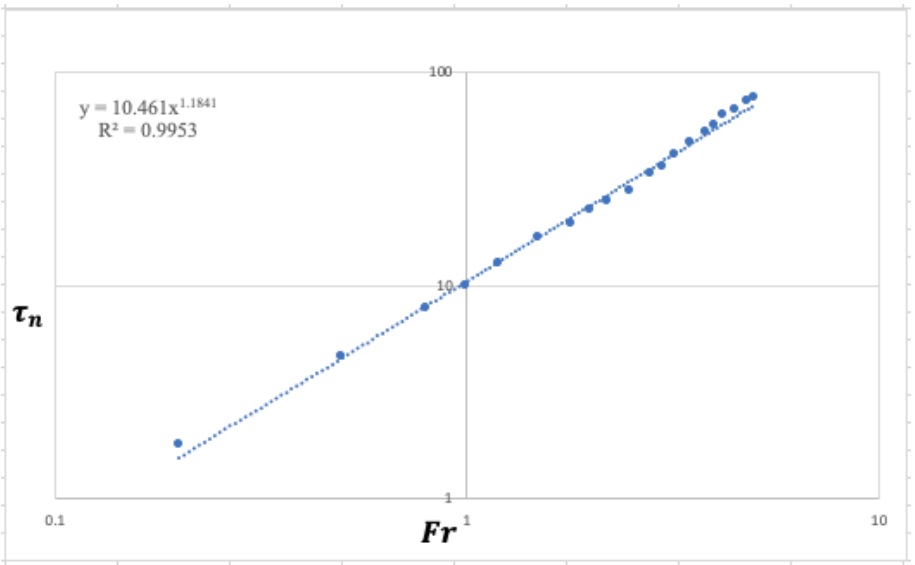


Fig. 14: Time taken for plume to reach maximum height, as a function of Froude number

higher Froude numbers, the detached head could penetrate farther, we are suggesting that much smaller values of Reynolds number and a moderate value of Froude number be reconsidered to know if these behaviours are entirely depended on flow parameters for the laminar flow scenario. Furthermore, higher Reynolds number should be investigated, both at transition to turbulence and in the fully turbulent case which is most relevant to environmental applications, with the aim of determining scalings of plume height against Reynolds number as found, for example, by Lin and Armfield [10]. Above all, we can conclude here that with the quadratic dependence relation assumption of density on temperature, and except for the behaviour in the profiles of vertical velocity component that show some slight differences as compared to those by [3] and the Froude number that represents the balance between inertia and buoyancy forces (responsible for the variation in the fountains heights). Irrespective of the flow parameters used within the Reynolds number range $50 \leq Re \leq 100$ and Prandtl number $Pr = 7 \,\&\, 11.4$ the flow behaviour remains the same.

## References

[1] Foster, T. D. (1972) *An analysis of the cabbeling instability in sea water. Journal of Physical Oceanography* **2***(3)* Pp. 294 - 301.

[2] George, M. A. and Kay, A. (2017). Numerical simulation of a line plume impinging on a ceiling in cold fresh water *International Journal of Heat and Mass Transfer* **108** Pp. 1364 - 1373.

[3] George, M. A. and Kay, A. (2017). Warm discharges in cold fresh water: 2. Numerical simulation of laminar line plumes *Environ. Fluid Mech* **17** Pp. 231 - 246.

[4] Macqueen, J. F. (1979) *Turbulence and cooling water discharges from power stations. In: Harris CJ (ed) Mathematical modelling of turbulent diffusion in the environment.* United Kingdom, Academic Press, London. Pp. 379 - 437

[5] Marmoush, Y. R., Smith, A. A. and Hamblin, P. F. (1984). Pilot experiments on thermal bar in lock exchange flow. *Journal of Energy Engineering - ASCE* **110** Pp. 215 - 227.

[6] Hoglund, B. and Spigarelli, S. A. (1972). Studies of the sinking plume phenomenon. In: Proceedings of the 15th conference on great lakes research. International Association of Great Lakes Research, Ann Arbor, Pp. 614 - 624.

[7] Bukreev, V. I. and Gusev, A. V. (2011). The effect of densification during mixing on the spreading of a vertical round jet *Doklady Earth Sciences* **439***(1)* Pp. 1002 - 1005.

[8] Lin, W. and Armfield, W. S. (2000). Direct simulation of weak axisymmetric fountains in a homogeneous fluid. *Journal of Fluid Mechanics* **403** Pp. 67 - 88.

[9] Lin, W. and Armfield, W. S. (2000). Direct simulation of weak laminar plane fountains in a homogeneous fluid. *International Journal of Heat and Mass Transfer* **43** Pp. 3013 - 3026.

[10] Lin, W. and Armfield, W. S. (2003). The Reynolds and Prandtl number dependence of weak fountains. *Comput Mech.* **31** Pp. 379 - 389.

[11] Srinarayana, N., McBain, D. G., Armfield, W. S. and Lin, W. (2008). Height and stability of laminar plane fountains in a homogeneous fluid. *International Journal of Heat and Mass Transfer* **51** Pp. 4717 - 4727.

[12] Srinarayana, N., Armfield, W. S. and Lin, W. (2013). Behaviour of laminar plane fountains with a parabolic inlet velocity profile in a homogeneous fluid. *International Journal of Therm Sci.* **67** Pp. 87 - 95.

[13] Srinarayana, N., Williamson, N., Armfield, W. S. and Lin, W. (2010). Line fountain behaviour at low Reynolds number. *International Journal of Heat and Mass Transfer* **53** Pp. 2065 - 2073.

[14] Williamson, N., Srinarayana, N., Armfield, W. S., McBain, D. G. and Lin, W. (2008). Low-Reynolds-number fountain behaviour. *Journal of Fluid Mech.* **608** Pp. 297 - 317.

[15] Burridge, H. C., Mistry, A. and Hunt, G. R. (2015). The effect of source Reynolds number on the rise height of a fountain. *Phys Fluids.* **27** Pp. 297 - 317.

[16] Caulfield, C-C. P. and Woods, A. W. (1995). Plumes with non-monotonic mixing behaviour. *Geophys Astrophys Fluid Dyn.* **79** Pp. 173 - 199.

[17] Morton B. R., Taylor, G. I. and Turner, J. S. (1956). Turbulent gravitational convection from maintained and instantaneous sources. *Proc R Soc Lond.* **234** Pp. 1 - 23.

[18] Kay, A. (2007). Warm discharges in cold fresh water: 1. Line plumes in a uniform ambient. *Journal of Fluid Mech.* **574** Pp. 239 - 271.

[19] Turner, J S. (1966). Jets and plumes with negative or reversing buoyancy. *Journal of Fluid Mech.* **26** Pp. 779 - 792.

[20] Moore, D. R. (1973). Nonlinear penetrative convection. *Journal of Fluid Mech.* **61** Pp. 553 - 581.

[21] Oosthuizen, P. H. (1996). A numerical study of the steady state freezing of water in an open rectangular cavity. *Int J Numer Meth Heat Fluid Flow.* **6** Pp. 3 - 16.

[22] COMSOL Multiphysics Cyclopedia. *The Finite Element Method (FEM). [ONLINE] Available at: https://www.comsol.com/multiphysics/finite-element-method [Accessed 28 April 2016].*

[23] Vinoth, B. R. and Panigrahi, P. K. (2014). Characteristics of low Reynolds number non-Boussinesq fountains from non-circular sources. *Phys Fluids.* **26** 014106.

[24] George, M. A. and Osaisai, F. E. (2022). A Numerical Study of the behaviour on Lock Volume Variations in Lock-Exchange Density Current In Cold Fresh Water. *Journal of Scientific Research & Reports* **28***(10)* Pp. 125 - 141.

[25] George, M. A. and Osaisai, F. E. (2022). Density Current Simulations In Cold Fresh Water And Its Cabbeling phenomenon: A Comparative Analysis With Given Experimental Results *Current Journal of Applied Science and Technology* **41***(29)* Pp. 37 - 52.

[26] George, M. A. and Osaisai, F. E. (2022). Propagation Speed of the Frontal Head Through Lock-Exchange Density Current in Cold Fresh Water: Simulations without the Effect of Back-reflected Waves *Asian Research Journal of Mathematics* **18***(11)* Pp. 249 - 260.

[27] Lin, W. and Armfield, W. S. (2000). Very weak fountains in a homogeneous fluid. *Numer Heat Transf A.* **38** Pp. 377 - 396.